NUKLEONIKA 2015;60(2):315–318
doi: 10.1515/nuka-2015-0065

ORIGINAL PAPER

DE GRUYTER
OPEN

Temporal distribution of linear densities of the plasma column in a plasma focus discharge

Balzhima Cikhardtova, Pavel Kubeš, Jakub Cikhardt, Marian Paduch, Ewa Zielinska, Josef Kravárik, Karel Řezáč, Jiři Kortanek, Ondřej Šíla

Abstract. Experiments were carried out on the PF-1000 plasma focus device, with a deuterium filling and with deuterium puffing from a gas-puff nozzle placed on the axis of the anode face. The current was reaching 2 MA. 15 interferometric frames from one shot were recorded with a Nd:YLF laser and a Mach–Zehnder interferometer, with 10–20 ns delay between the frames. As a result, the temporal and spatial distribution of the linear densities and the radial and axial velocities of the moving of plasma in the dense plasma column could be estimated.

Key words: plasma focus (PF) • plasma pinch • plasma diagnostics

B. Cikhardtova✉, P. Kubeš, J. Cikhardt, J. Kravárik, K. Řezáč, J. Kortanek, O. Šíla
Faculty of Electrical Engineering,
Czech Technical University in Prague,
Technicka 2, 166 27 Prague 6, Czech Republic,
E-mail: batobbal@fel.cvut.cz

M. Paduch, E. Zielinska
Institute of Plasma Physics and Laser Microfusion (IPPLM),
23 Hery Str., 01-497 Warsaw, Poland

Received: 8 June 2014
Accepted: 18 February 2015

Introduction

Plasma focus devices and Z-pinches have wide application because they are highly efficient and cost effective technique to heat a small mass to a very high temperature. They have been used widely to produce X-rays [1] or fusion neutrons on the facilities operating with deuterium.

The deuterium plasma has been studied at the PF-1000 facility with using a multiframe interferometry [2–5], which allows for the distribution of the deuterium plasma in the plasma column to be estimated. In this paper experimental results on the transport of the plasma in the transverse direction and the z direction are presented.

Description of the experimental setup and diagnostics

Experiments were carried out on the PF-1000 plasma focus facility equipped with the Mather-type coaxial electrodes 48 cm in length. The anode diameter was 23 cm. The cathode 40 cm in diameter was composed of twelve stainless-steel rods 82 mm in diameter distributed symmetrically around the anode circumference. The condenser bank was charged to the voltage of 23 kV, which corresponded to discharge energies of 350 kJ. The maximal discharge current amounted to 1.7–1.9 MA. The initial pressure in the discharge chamber with a deuterium filling was about 200 Pa [6].

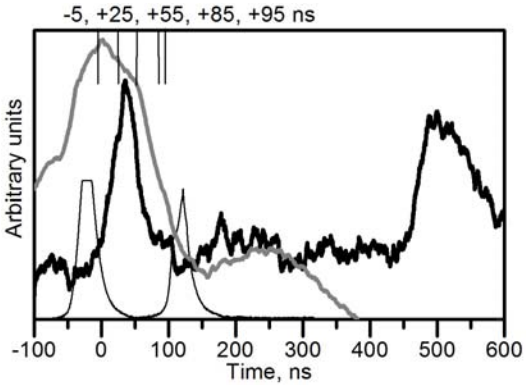

Fig. 1. Shot #9881. Signals from PIN (black thin), HXR and neutrons (thick black line) and the time derivative of the current (thick gray line).

The voltage, time derivative of the current and the current were measured within the current collector near the insulator at the bottom of the anode. To determine the time at which hard X-rays (HXRs) and neutrons were generated three scintillation detectors were used, coupled with fast photomultipliers situated in side-on, downstream and upstream directions at the distances of 7 m. A soft X-ray (SXR) signal of the photon energy of 0.7–15 keV was recorded by the silicon PIN detector. The interferometric measurements were performed with a Nd:YLF laser operated at the second harmonics (527 nm). The laser pulse (shorter than 1 ns) was split by a set of mirrors into fifteen separate beams, which passed through a Mach–Zehnder interferometer. These beams probed the plasma region at 10–20 ns intervals over the period of 210 ns [2]. The time scale was adjusted in such a way that the moment of t = 0 corresponded to the minimum of the derivative of the current. The uncertainty in timing of different signals was about 2–3 ns.

Experimental results

In this paper, the shot #9881 is analyzed. Signals of SXRs, HXRs, neutrons in radial direction and time derivative of the current are shown in Fig. 1. Three interferograms registered at –5 ns, +55 ns and +95 ns are shown in Fig. 2.

In order to calculate the electron density the relation between the phase (i.e. the number of shifted fringes) and the electron density [m^{-3}] in fully ionized plasma was used [7]:

$$\delta = -4.5\times10^{-16}\lambda\int_0^l n_e(x,y,z)dl \quad (1)$$

where δ is the number of shifted fringes, λ [m] is the wavelength of the laser beam, l [m] is length of the laser path in plasma, and n_e is the electron density.

The distribution of the linear density $N(x,z)$ is calculated along the laser beam (y-axis) in every square $\Delta x \cdot \Delta z$:

$$N(x,z) = \Delta x\cdot\Delta z\int_0^l n_e(x,y,z)dl = \Delta x\cdot\Delta z\frac{\delta}{4.5\times10^{-16}\lambda} \quad (2)$$

Assuming Δx = 0.5 mm, Δz = 1 mm, and λ = 527 nm, the formula for the distribution of the linear density takes the following form:

$$N(x,z) = \delta\cdot 2.1\times10^{15} \quad (3)$$

The distribution of the linear density $N(x,z)$ for different z-levels at –5 and +25 ns is shown in Fig. 3. For t = –5 ns the maxima of $N(x,z)$ are close to the plasma column boundary. For t = +25 ns (Fig. 3b) the maxima of $N(x,z)$ on each z-level move towards the center of the plasma column. The radii of the pinch column are decreasing along the whole z-axis. The zipper effect along the z-axis is well visible. The velocity of zippering is (5–15) × 10^5 m/s.

The maxima of $N(x,z)$ at each z-level are located in the center of the plasma column at +55 ns (Fig. 4a). The radii of the plasma column are slowly increasing at the lower values of z.

At +85 ns and z = 45 mm (Fig. 4b) the radius of the plasma column is still decreasing, while at z = 40 mm the radius of the column is already increasing. The maxima of $N(x,z)$ are decreasing along the total z-axis.

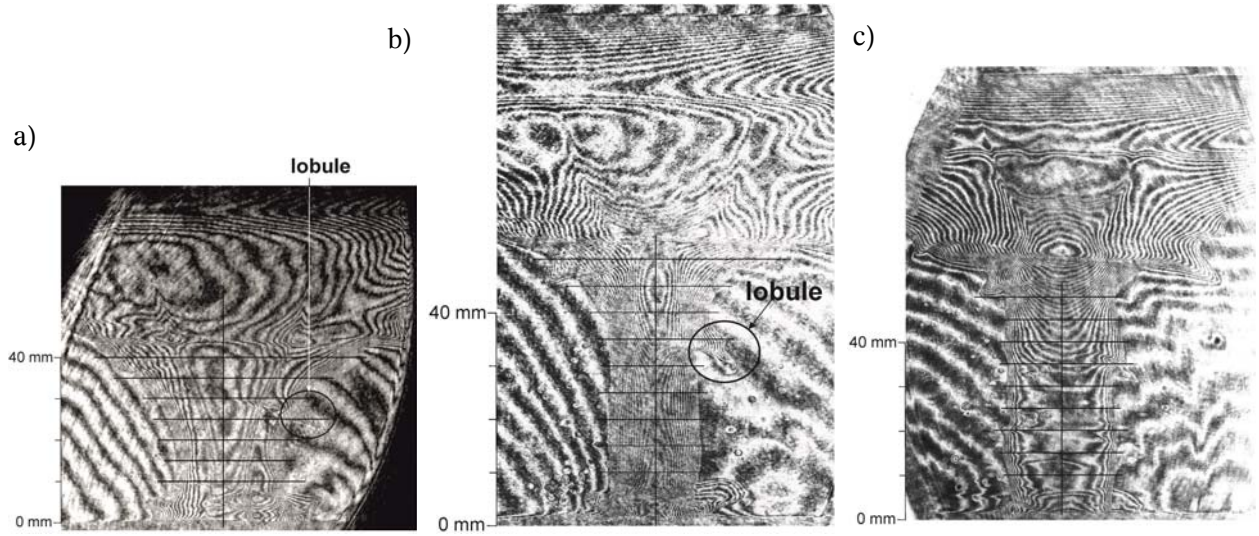

Fig. 2. Interferograms at –5 ns (a), +55 ns (b) and +95 ns (c).

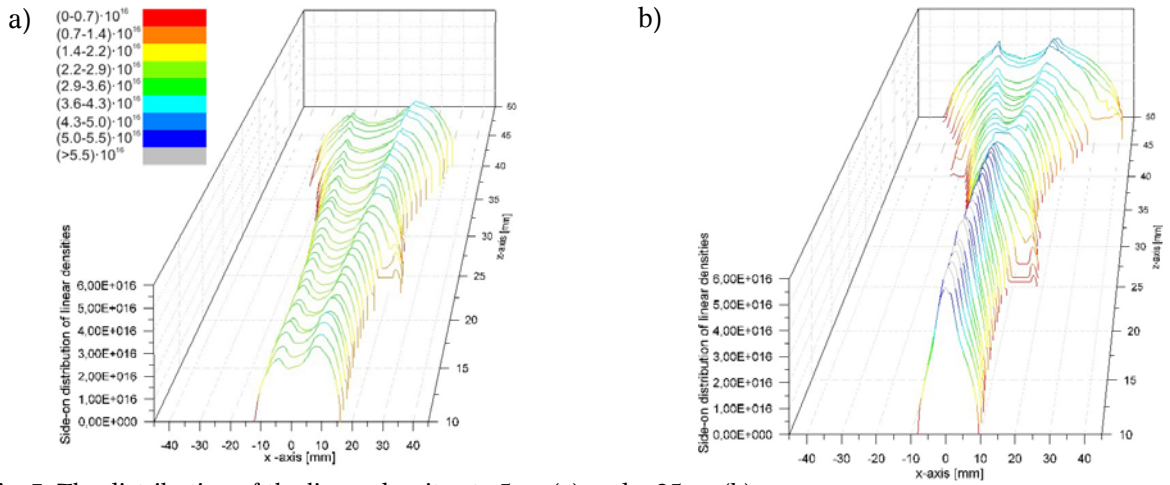

Fig. 3. The distribution of the linear density at –5 ns (a) and +25 ns (b).

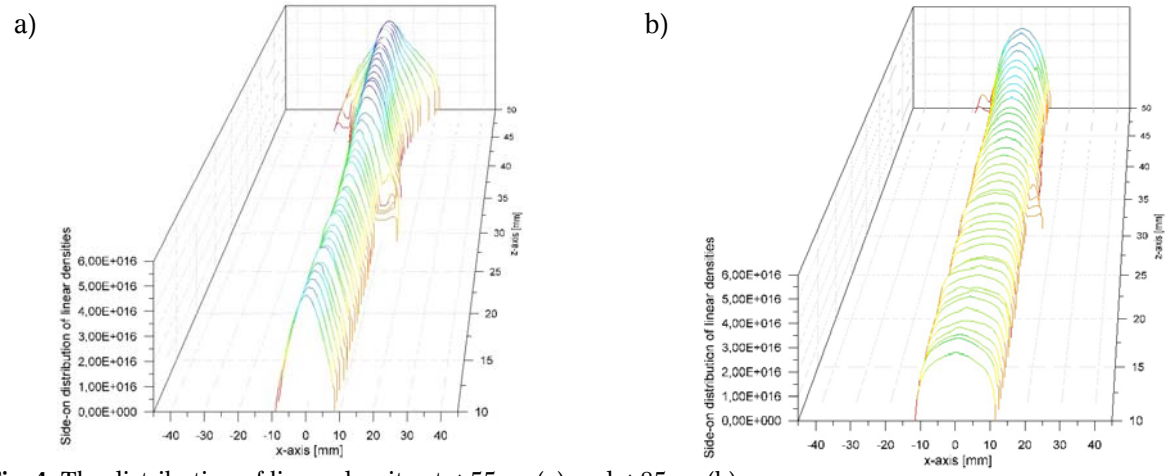

Fig. 4. The distribution of linear density at +55 ns (a) and +85 ns (b).

For t = +95 ns (Fig. 5) the maxima of $N(x,z)$ are continuing to decrease along the whole z-axis. This is due to the elongation of the plasma column.

The curves representing the linear density of plasma $N(z)$ for different instants of time are shown in Fig. 6. For lower values of z the linear densities decrease more slowly than for the higher values of z. The linear density decreases down to the value of 0.8×10^{18} per mm with z in the range of 10–34 mm for t = +95 ns. It is seen from Figs. 3–6 that part of plasma is redistributed in the axial as well as in the radial directions.

In Fig. 6 we see a small peak at z = 25 mm and –5 ns, then at z = 30 mm and +25 ns and then at z = 35 mm and +55 ns. It is caused by the lobule (Fig. 2a) moving along the z-axis and transporting some amount of plasma. In this shot, the velocity of this axial motion of the lobule is about $(1.5 \pm 0.3) \times 10^5$ m/s.

The linear densities at –5 ns have higher values than at later times. This is explained by the effect

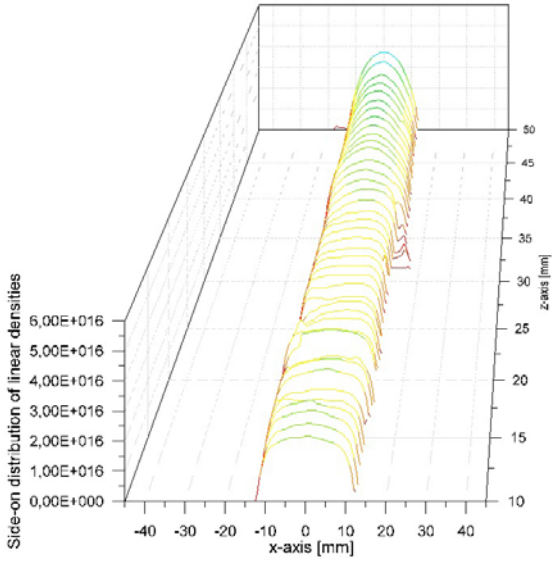

Fig. 5. The distribution of the linear density at +95 ns.

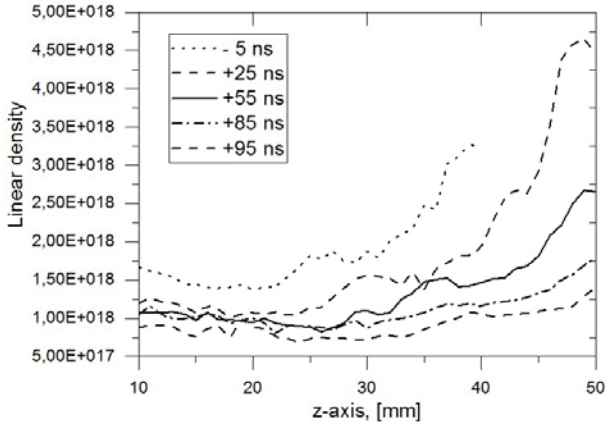

Fig. 6. The temporal evolution of the linear density.

of transport of plasma along the z-axis during its elongation.

Summary and conclusions

The conclusions can be summarized as follows:

1. In this paper, the axial and radial motion of some part of plasma in the plasma column is imaged.
2. The plasma boundary moves in the radial direction towards the z-axis during the implosion and then plasma expands. The mean velocity of the implosion is $(2.2 \pm 0.4) \times 10^5$ m/s. The velocity of the expansion grows from 0.4×10^5 m/s to 1.2×10^5 m/s.
3. The mean velocity of transport of the plasma structures along the z-axis is $(1.5 \pm 0.3) \times 10^5$ m/s. The velocity of the zippering is (5–15) $\times 10^5$ m/s.

Acknowledgment. This work was supported in part by the research program under grants MSMT no. LG13029, LH13283, GACR P205/12/0454, IAEA RC-16115, RC-16954, RC-16956, RC-17088 and SGS 10/266/OHK3/3T/13 as well as national resources allocated to science in 2014, awarded to support co-financed international collaborative projects.

References

1. Liberman, M. A., De Groot, J. S., Toor, A., & Spielman, R. B. (1999). *Physics of high-density Z-pinch plasmas*. New York: Springer.
2. Zielinska, E., Paduch, M., & Scholz, M. (2011). Sixteen-frame interferometer for a study of a pinch dynamics in PF-1000 device. *Conrib. Plasma Phys.*, *51*, 279.
3. Paduch, M. (2009). *The diagnostics problems at implementation of Plasma Focus technique in material and environmental sciences*, Tallinn University Dissertations on Natural Sciences, Tallinn.
4. Kubes, P., Klir, D., Kravarik, J., Rezac, K., Kortanek, J., Krauz, V., Mitrofanov, K., Paduch, M., Scholz, M., Pisarczyk, T., Chodukowski, T., Kalinowska, Z., Karpinski, L., & Zielinska, E. (2013). Scenario of pinch evolution in a plasma focus discharge. *Plasma Phys. Control. Fusion*, *55*, 035011.
5. Kubes, P., Paduch, M., Pisarczyk, T., Scholz, M., Chodukowski, T., Klir, D., Kravarik, J., Rezac, K., Ivanova-Stanik, I., Karpinski, L., Tomaszewski, K., & Zielinska, E. (2009). Interferometric study of pinch phase in Plasma-Focus discharge at the time of neutron production. *IEEE Trans. Plasma Sci*., *37*, 11.
6. Kubes, P., Paduch, M., Cikhardt, J., Kortanek, J., Batobolotova, B., Rezac, K., Klir, D., Kravarik, J., Surala, W., Zielinska, E., Scholz, M., Karpinski, L., & Sadowski, M. J. (2014). Neutron production from puffing deuterium in plasma focus device. *Phys. Plasmas*, *21*, 082706.
7. Dolgov-Savelyev, G. G., Kruglyakov, E. P., Malinovskij, V. K., & Fedorov, V. M. (1968). *Diagnostika plazmy*. Moscow: Atomizdat.